Measurement and analysis of muonic x rays of ^{176,177,178,179,180}Hf

Y. Tanaka and R. M. Steffen
Department of Physics, Purdue University, West Lafayette, Indiana 47907

E. B. Shera, W. Reuter, and M. V. Hoehn
Los Alamos National Laboratory, Los Alamos, New Mexico 87545

J. D. Zumbro
Department of Physics, Princeton University, Princeton, New Jersey 08544

(Received 26 January 1984)

Monopole and quadrupole charge distributions of ^{176}Hf, ^{177}Hf, ^{178}Hf, ^{179}Hf, and ^{180}Hf were investigated by muonic atom K and L x-ray measurements. The model-independent Barrett charge radii R_k and the isotope shifts ΔR_k were measured, and values of $\langle r^2\rangle$ and $\Delta\langle r^2\rangle$ were deduced. A weak odd-even staggering of the nuclear charge radii was observed for the series $^{176-178}$Hf and $^{178-180}$Hf. A large negative isomer shift was observed in the 2^+ state of the ^{176}Hf nucleus, a fact that existing theories do not explain. The quadrupole moments of the first excited states of the hafnium nuclei were determined to be $Q^{176}(2^+)=-2.10(2)\ e$ b, $Q^{177}(\frac{9}{2}^-)=1.30(2)\ e$ b, $Q^{178}(2^+)=-2.02(2)\ e$ b, $Q^{179}(\frac{11}{2}^+)=1.88(3)\ e$ b, and $Q^{180}(2^+)=-2.00(2)\ e$ b. These quadrupole moments and the simultaneously determined $B(E2)$ values for the respective nuclei are in satisfactory agreement with the predictions of the axially symmetric rotor model.

I. INTRODUCTION

Nuclei in the mass number $A=150-190$ region begin with the axially symmetric deformed rotors of samarium and gadolinium and end with the γ-soft deformed rotors of osmium. The stable isotopes of hafnium have fairly large deformation parameters ($\beta_2\simeq 0.26$) and relatively high γ vibrational bands (~ 1.2 MeV). It is therefore reasonable to expect that these nuclei, like samarium and gadolinium, are axially symmetric rotors.

However, the hafnium nuclei are located in the region where β_2 starts to decrease[1,2] and by implication the tendency toward γ softness begins. Hence it is of interest to investigate the shapes of the hafnium nuclei by determining with high precision the isotope shifts, isomer shifts, quadrupole moments, and $B(E2)$ values of their low-lying states. Measurements of the energies of muonic x rays are particularly well suited for such an investigation.

II. MEASUREMENTS AND EXPERIMENTAL RESULTS

The muonic x-ray spectra of $^{176-180}$Hf were measured at the Los Alamos Meson Physics Facility. The target arrangement, Ge(Li) spectrometer, and data-acquisition system have been described in detail in previous papers.[3,4] The muonic x-ray spectrum from a target of ^{208}Pb was recorded simultaneously with the hafnium data for energy calibration. The γ-ray spectra from ^{24}Na, ^{56}Co, ^{110}Ag, ^{182}Ta, ^{198}Au, and ^{208}Pb were also measured in a separate run to determine the nonlinearity of the data-acquisition system.

The masses and isotopic compositions of the hafnium targets are listed in Table I. The raw spectra were corrected by subtracting the appropriate fractions of the spectra of the impurity isotopes. The impurity-corrected K and L x-ray spectra are shown in Figs. 1–4. The spectra were directly fitted[5] by distributions constructed from theoretical x-ray energy and intensity patterns that were convoluted with the known response function of the Ge(Li) detector. The detector response was represented by a Gaussian-convoluted Lorentzian with exponential tails, for which the Lorentzian widths were computed from the natural linewidths of the transitions, and the exponential tail parameters were determined by fitting the K, L, and M x-ray spectra of muonic ^{208}Pb. The fitted theoretical function and the fitted quadratic background is shown in each of the figures. For the even-A isotopes the relative

TABLE I. Isotopic compositions of the hafnium targets.

Target	Mass of Hf (g)	Isotopic composition (%) 176	177	178	179	180
^{176}Hf	8.84	68.7	14.9	8.68	2.73	4.99
^{177}Hf	4.59	1.20	86.49	7.47	1.71	3.11
^{178}Hf	7.40	0.24	1.55	94.59	1.90	1.72
^{179}Hf	3.43	0.18	1.03	3.26	86.98	8.55
^{180}Hf	20.03	0.23	1.0	2.22	2.66	93.89

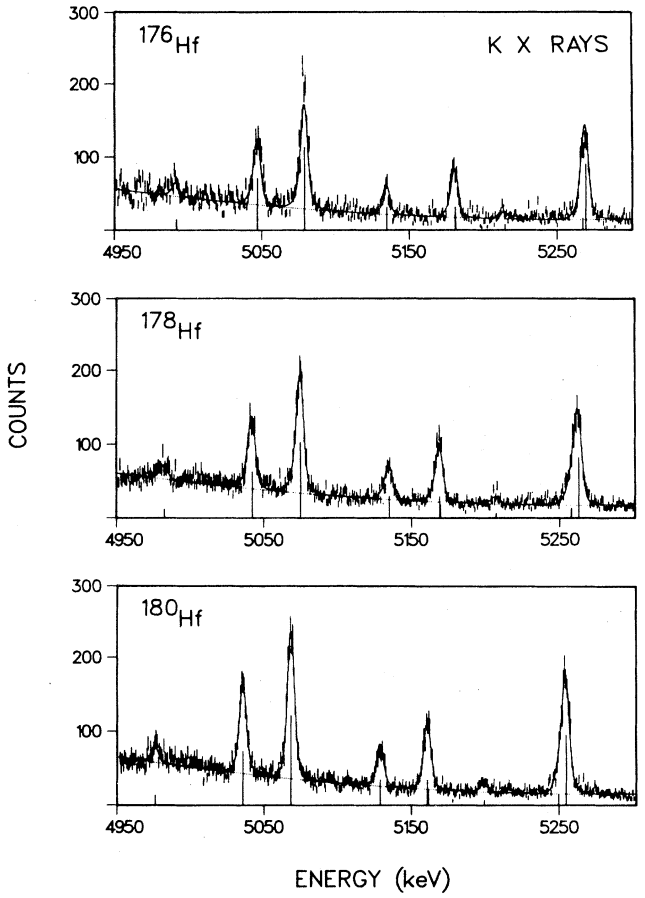

FIG. 1. The muonic K x-ray spectra of ^{176}Hf, ^{178}Hf, and ^{180}Hf. The solid curve represents the best-fit theoretical spectrum. The vertical lines show the calculated transition energies and intensities.

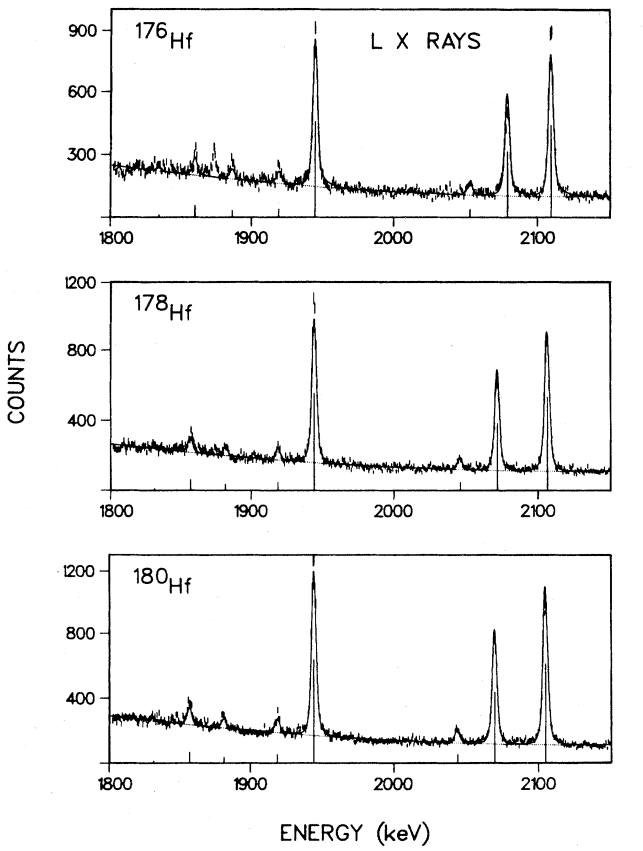

FIG. 2. The muonic L x-ray spectra of ^{176}Hf, ^{178}Hf, and ^{180}Hf. The solid curve represents the best-fit theoretical spectrum. The vertical lines show the calculated transition energies and intensities.

simplicity of the spectra made it possible to also use the conventional method of fitting individual lines.[4] In this case the fitting function was composed of a quadratic background and a Gaussian-convoluted Lorentzian with exponential tails. Table II displays the x-ray transition energies and intensities for the even-A isotopes that resulted from this fitting procedure.

The energy calibration was based on a linear interpolation of the observed channel positions of the muonic x-ray lines of ^{208}Pb. The K x-ray energies were taken from Kessler *et al.*,[6] and the L and M x-ray energies were taken from a new Los Alamos measurement.[7]

III. ANALYSIS OF THE MUONIC X-RAY SPECTRA

Muonic x-ray measurements can provide monopole and quadrupole charge parameters of the nuclear ground state and of those nuclear states that mix reasonably strongly with the muonic states populated in the deexcitation of the muonic atom. Analysis of the even-A hafnium spectra involved only the ground state, the first 2^+ state, and the first 4^+ state, and analysis of the odd-A hafnium

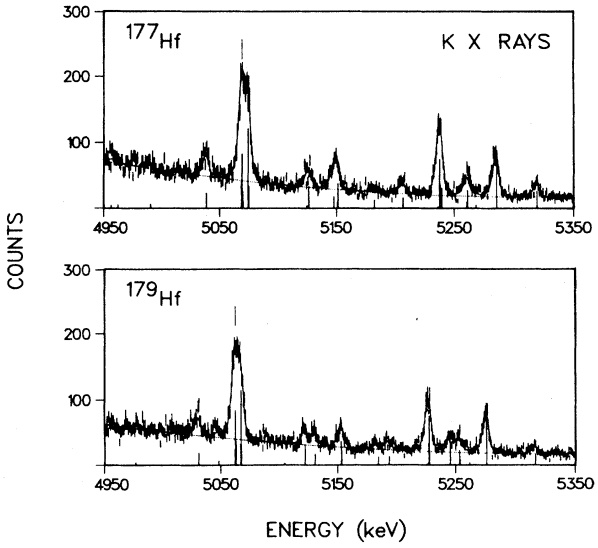

FIG. 3. The muonic K x-ray spectra of ^{177}Hf and ^{179}Hf. The solid curve represents the best-fit theoretical spectrum. The vertical lines show the calculated transition energies and intensities.

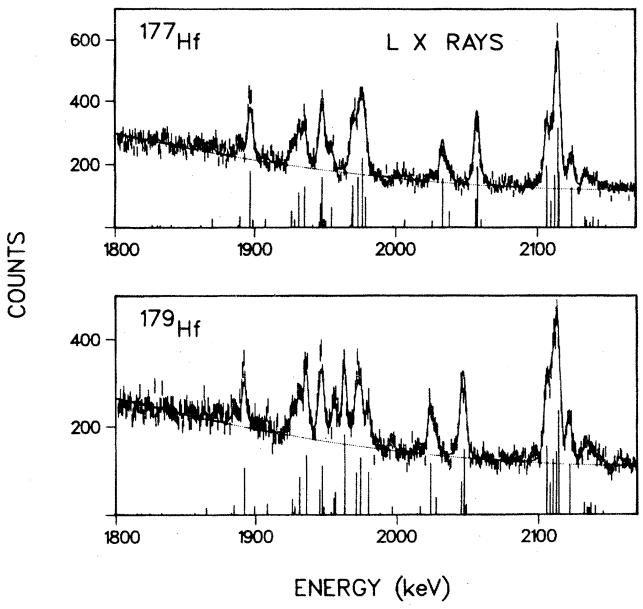

FIG. 4. The muonic L x-ray spectra of ^{177}Hf and ^{179}Hf. The solid curve represents the best-fit theoretical spectrum. The vertical lines show the calculated transition energies and intensities.

spectra involved the ground state and the ground-state rotational band members up to the fourth excited states. Although several low-lying excited-state rotational bands exist in these isotopes (e.g., the $\frac{9}{2}[624]$ rotational band in ^{177}Hf and the $\frac{7}{2}[514]$ and $\frac{1}{2}[510]$ rotational bands in ^{179}Hf), their contribution to the muonic spectra can be neglected because of parity considerations.

The nuclear electric monopole and quadrupole parameters were extracted following the procedure outlined in Ref. 8. The nuclear monopole and quadrupole charge densities were constructed from a multipole expansion of the deformed Fermi charge distribution [see Eq. (22) in Ref. 4]. The quadrupole deformation parameters β_2 were computed for the even-A nuclei from the rotational model and $B(E2{:}0^+\rightarrow 2^+)$ values,[1] and for the odd-A nuclei from the ground-state quadrupole-moment values.[2] The hexadecapole deformation parameters β_4 were assumed to be zero.

The muonic-atom binding energies and eigenfunctions were computed numerically for the various isotopes with the computer program MUON2,[9] which is based on the program MUON of Rinker.[10] The binding energies were corrected, following Ref. 11, for vacuum polarization effects, self-energy effects (Lamb shift), electron screening, and relativistic recoil. The corrections also included the

TABLE II. Experimental and calculated energies and intensities of the x-ray transitions of muonic ^{176,178,180}Hf. The errors listed for the experimental energies and relative intensities include only statistical errors and uncertainties of the calibration energies. The calculated energies and relative intensities were obtained by using nuclear parameters adjusted to best fit the experimental transition energies. The goodness of fit is indicated by the χ^2 values of 18.7, 3.9, and 6.9 for ^{176}Hf, ^{178}Hf, and ^{180}Hf, respectively.

	Transition		Experimental		Calculated	
Nucleus	Initial state (Major component)	Final state	Energy (keV)	Relative intensity	Energy (keV)	Relative intensity
^{176}Hf	$\|0^+\times 2p_{3/2};\frac{3}{2}^-\rangle$	$\|0^+\times 1s_{1/2};\frac{1}{2}^+\rangle$	5268.95(23)	0.238(11)	5269.25	0.224
	$\|2^+\times 2p_{3/2};\frac{3}{2}^-\rangle$	$\|2^+\times 1s_{1/2};\frac{3}{2}^+\rangle$			5267.23	0.040
	$\|2^+\times 2p_{3/2};\frac{1}{2}^-\rangle$	$\|2^+\times 1s_{1/2};\frac{3}{2}^+\rangle$	5214.21(73)	0.020(4)	5215.04	0.020
	$\|0^+\times 2p_{3/2};\frac{3}{2}^-\rangle$	$\|2^+\times 1s_{1/2};\frac{3}{2}^+\rangle$	5181.17(26)	0.128(7)	5181.90	0.054
	$\|0^+\times 2p_{3/2};\frac{3}{2}^-\rangle$	$\|2^+\times 1s_{1/2};\frac{5}{2}^+\rangle$			5181.42	0.078
	$\|2^+\times 2p_{1/2};\frac{3}{2}^-\rangle$	$\|0^+\times 1s_{1/2};\frac{1}{2}^+\rangle$	5134.82(36)	0.062(6)	5135.10	0.079
	$\|0^+\times 2p_{1/2};\frac{1}{2}^-\rangle$	$\|0^+\times 1s_{1/2};\frac{1}{2}^+\rangle$	5079.41(21)	0.321(13)	5079.29	0.280
	$\|2^+\times 2p_{1/2};\frac{3}{2}^-\rangle$	$\|2^+\times 1s_{1/2};\frac{5}{2}^+\rangle$	5047.87(24)	0.188(10)	5047.27	0.175
	$\|0^+\times 2p_{1/2};\frac{1}{2}^-\rangle$	$\|2^+\times 1s_{1/2};\frac{3}{2}^+\rangle$	4991.11(56)	0.044(6)	4991.94	0.036
	$\|0^+\times 3d_{3/2};\frac{3}{2}^+\rangle$	$\|0^+\times 2p_{1/2};\frac{1}{2}^-\rangle$	2109.30(5)	0.352(8)	2109.30	0.316
	$\|0^+\times 3d_{5/2};\frac{5}{2}^+\rangle$	$\|2^+\times 2p_{1/2};\frac{3}{2}^-\rangle$	2079.27(6)	0.193(5)	2079.23	0.225
	$\|0^+\times 3d_{3/2};\frac{3}{2}^+\rangle$	$\|2^+\times 2p_{1/2};\frac{3}{2}^-\rangle$	2053.38(24)	0.029(3)	2053.49	0.028
	$\|0^+\times 3d_{5/2};\frac{5}{2}^+\rangle$	$\|0^+\times 2p_{3/2};\frac{3}{2}^-\rangle$	1945.04(5)	0.317(8)	1945.08	0.329
	$\|0^+\times 3d_{3/2};\frac{3}{2}^+\rangle$	$\|0^+\times 2p_{3/2};\frac{3}{2}^-\rangle$	1919.50(25)	0.032(3)	1919.34	0.027
	$\|0^+\times 3d_{3/2};\frac{3}{2}^+\rangle$	$\|2^+\times 2p_{3/2};\frac{1}{2}^-\rangle$	1886.20(25)	0.035(3)	1886.20	0.022
	$\|0^+\times 3d_{5/2};\frac{5}{2}^+\rangle$	$\|2^+\times 2p_{3/2};\frac{3}{2}^-\rangle$	1860.11(21)	0.042(4)	1859.75	0.040
^{178}Hf	$\|0^+\times 2p_{3/2};\frac{3}{2}^-\rangle$	$\|0^+\times 1s_{1/2};\frac{1}{2}^+\rangle$	5262.65(27)	0.213(12)	5262.59	0.226
	$\|2^+\times 2p_{3/2};\frac{3}{2}^-\rangle$	$\|2^+\times 1s_{1/2};\frac{3}{2}^+\rangle$	5257.86(27)	0.062(11)	5257.79	0.036

TABLE II. (*Continued*).

Nucleus	Transition: Initial state (Major component)	Transition: Final state	Experimental: Energy (keV)	Experimental: Relative intensity	Calculated: Energy (keV)	Calculated: Relative intensity
	$\|2^+\times 2p_{3/2};\frac{1}{2}^-\rangle$	$\|2^+\times 1s_{1/2};\frac{3}{2}^+\rangle$	5207.91(89)	0.016(4)	5207.14	0.018
	$\|0^+\times 2p_{3/2};\frac{3}{2}^-\rangle$	$\|2^+\times 1s_{1/2};\frac{3}{2}^+\rangle$	5169.38(24)	0.143(8)	5169.87	0.050
	$\|0^+\times 2p_{3/2};\frac{3}{2}^-\rangle$	$\|2^+\times 1s_{1/2};\frac{5}{2}^+\rangle$			5169.44	0.082
	$\|2^+\times 2p_{1/2};\frac{3}{2}^-\rangle$	$\|0^+\times 1s_{1/2};\frac{1}{2}^+\rangle$	5135.33(32)	0.071(6)	5135.15	0.083
	$\|0^+\times 2p_{1/2};\frac{1}{2}^-\rangle$	$\|0^+\times 1s_{1/2};\frac{1}{2}^+\rangle$	5075.00(21)	0.288(12)	5075.11	0.286
	$\|2^+\times 2p_{1/2};\frac{3}{2}^-\rangle$	$\|2^+\times 1s_{1/2};\frac{5}{2}^+\rangle$	5042.13(24)	0.163(9)	5042.00	0.174
	$\|0^+\times 2p_{1/2};\frac{1}{2}^-\rangle$	$\|2^+\times 1s_{1/2};\frac{3}{2}^+\rangle$	4982.27(55)	0.044(6)	4982.38	0.033
	$\|0^+\times 3d_{3/2};\frac{3}{2}^+\rangle$	$\|0^+\times 2p_{1/2};\frac{1}{2}^-\rangle$	2106.26(5)	0.302(7)	2106.26	0.319
	$\|0^+\times 3d_{5/2};\frac{5}{2}^+\rangle$	$\|2^+\times 2p_{1/2};\frac{3}{2}^-\rangle$	2071.97(5)	0.211(5)	2071.96	0.229
	$\|0^+\times 3d_{3/2};\frac{3}{2}^+\rangle$	$\|2^+\times 2p_{1/2};\frac{3}{2}^-\rangle$	2046.12(25)	0.026(2)	2046.22	0.028
	$\|0^+\times 3d_{5/2};\frac{5}{2}^+\rangle$	$\|0^+\times 2p_{3/2};\frac{3}{2}^-\rangle$	1944.50(4)	0.367(8)	1944.51	0.330
	$\|0^+\times 3d_{3/2};\frac{3}{2}^+\rangle$	$\|0^+\times 2p_{3/2};\frac{3}{2}^-\rangle$	1919.01(27)	0.028(3)	1918.78	0.027
	$\|0^+\times 3d_{3/2};\frac{3}{2}^+\rangle$	$\|2^+\times 2p_{3/2};\frac{1}{2}^-\rangle$	1881.69(37)	0.021(3)	1881.50	0.020
	$\|0^+\times 3d_{5/2};\frac{5}{2}^+\rangle$	$\|2^+\times 2p_{3/2};\frac{3}{2}^-\rangle$	1857.33(19)	0.045(3)	1856.59	0.035
^{180}Hf	$\|0^+\times 2p_{3/2};\frac{3}{2}^-\rangle$	$\|0^+\times 1s_{1/2};\frac{1}{2}^+\rangle$	5254.70(24)	0.235(10)	5254.63	0.227
	$\|2^+\times 2p_{3/2};\frac{3}{2}^-\rangle$	$\|2^+\times 1s_{1/2};\frac{3}{2}^+\rangle$	5249.76(24)	0.035(7)	5249.73	0.035
	$\|2^+\times 2p_{3/2};\frac{1}{2}^-\rangle$	$\|2^+\times 1s_{1/2};\frac{3}{2}^+\rangle$	5199.27(61)	0.020(3)	5199.66	0.017
	$\|0^+\times 2p_{3/2};\frac{3}{2}^-\rangle$	$\|2^+\times 1s_{1/2};\frac{3}{2}^+\rangle$	5161.35(24)	0.133(7)	5161.71	0.050
	$\|0^+\times 2p_{3/2};\frac{3}{2}^-\rangle$	$\|2^+\times 1s_{1/2};\frac{5}{2}^+\rangle$			5161.25	0.082
	$\|2^+\times 2p_{1/2};\frac{3}{2}^-\rangle$	$\|0^+\times 1s_{1/2};\frac{1}{2}^+\rangle$	5129.27(30)	0.071(5)	5129.17	0.082
	$\|0^+\times 2p_{1/2};\frac{1}{2}^-\rangle$	$\|0^+\times 1s_{1/2};\frac{1}{2}^+\rangle$	5068.50(20)	0.291(11)	5068.59	0.288
	$\|2^+\times 2p_{1/2};\frac{3}{2}^-\rangle$	$\|2^+\times 1s_{1/2};\frac{5}{2}^+\rangle$	5035.70(22)	0.178(8)	5035.78	0.174
	$\|0^+\times 2p_{1/2};\frac{1}{2}^-\rangle$	$\|2^+\times 1s_{1/2};\frac{3}{2}^+\rangle$	4976.65(54)	0.037(5)	4975.67	0.032
	$\|0^+\times 3d_{3/2};\frac{3}{2}^+\rangle$	$\|0^+\times 2p_{1/2};\frac{1}{2}^-\rangle$	2104.91(5)	0.295(6)	2104.94	0.319
	$\|0^+\times 3d_{5/2};\frac{5}{2}^+\rangle$	$\|2^+\times 2p_{1/2};\frac{3}{2}^-\rangle$	2070.10(5)	0.213(5)	2070.08	0.228
	$\|0^+\times 3d_{3/2};\frac{3}{2}^+\rangle$	$\|2^+\times 2p_{1/2};\frac{3}{2}^-\rangle$	2044.47(19)	0.029(2)	2044.35	0.028
	$\|0^+\times 3d_{5/2};\frac{5}{2}^+\rangle$	$\|0^+\times 2p_{3/2};\frac{3}{2}^-\rangle$	1944.63(4)	0.356(7)	1944.62	0.332
	$\|0^+\times 3d_{3/2};\frac{3}{2}^+\rangle$	$\|0^+\times 2p_{3/2};\frac{3}{2}^-\rangle$	1919.00(20)	0.032(3)	1918.89	0.028
	$\|0^+\times 3d_{3/2};\frac{3}{2}^+\rangle$	$\|2^+\times 2p_{3/2};\frac{1}{2}^-\rangle$	1880.64(26)	0.026(3)	1880.95	0.019
	$\|0^+\times 3d_{5/2};\frac{5}{2}^+\rangle$	$\|2^+\times 2p_{3/2};\frac{3}{2}^-\rangle$	1856.62(15)	0.050(3)	1856.61	0.035

effects of the quadrupole vacuum polarization.[12]

With the muonic wave functions so obtained, we computed the matrix elements of the interaction Hamiltonian $H_{\mu N}=H(E2)+H(M1)$ that describes the electric quadrupole and magnetic dipole interactions with the relevant nuclear states. As mentioned above, the muon-nuclear interaction $H_{\mu N}$ was diagonalized in the space that included the 0^+, 2^+, and 4^+ nuclear states for the even-A isotopes, the $\frac{7}{2}^-$, $\frac{9}{2}^-$, $\frac{11}{2}^-$, $\frac{13}{2}^-$, and $\frac{15}{2}^-$ states for ^{177}Hf, and the $\frac{9}{2}^+$, $\frac{11}{2}^+$, $\frac{13}{2}^+$, $\frac{15}{2}^+$, and $\frac{17}{2}^+$ states for ^{179}Hf. The effects of the muonic states that were not explicitly included in the model space were taken into account by nuclear polarization corrections.[9] Values of the nuclear parameters that were held fixed in the analysis are listed in Tables III and IV. These fixed parameters were either taken from the literature or computed from the experimental quadrupole moments using the rotational model.

In the analysis of the even-A hafnium spectra, the radius and the diffuseness parameters of the deformed Fermi charge distribution, the matrix elements $\langle 2^+||r^2Y_2||2^+\rangle$ and $\langle 2^+||r^2Y_2||0^+\rangle$, and the isomer-shift energy $\Delta E_{\rm iso}$ of the 2^+ excited state were adjusted

TABLE III. Parameters fixed in the analysis of data for even-A hafnium nuclei.

	^{176}Hf	^{178}Hf	^{180}Hf
β_2[a]	0.270	0.259	0.254
$E(2^+)$ (keV)	88.35	93.17	93.324
$E(4^+)$ (keV)	290.2	306.60	308.58
$\mu(2^+)$[b] (μ_N)	0.54	0.48	0.53
$Q(4^+)$[a] (e b)	−2.63	−2.54	−2.51
$B(E2{:}2^+\rightarrow 4^+)$[a] ($e^2b^2$)	2.67	2.50	2.44

[a]Computed from the experimental $B(E2{:}0^+\rightarrow 2^+)$ values of Ref. 1 using the rotational model.
[b]*Table of Isotopes,* 7th ed., edited by C. M. Lederer and V. S. Shirley (Wiley, New York, 1977).

simultaneously to best reproduce the observed muonic K and L x-ray spectra. For the odd-A hafnium nuclei, the radius and the diffuseness parameters of the charge distribution, the quadrupole matrix elements of the ground state and of the lowest two excited states, and the isomer-shift energy ΔE_{iso} of the first excited state were adjusted to best fit the observed spectra. Cascade calculations involved in this fitting procedure started from the muonic $4f$ states. For each coupled muon-nuclear state with a total angular momentum F, we assumed a statistical population proportional to $2F+1$.

The quality of the fits (shown in Figs. 1—4) indicates the adequacy of our theoretical representation for the experimental K and L x-ray spectra. It also indicates that statistical population of the $4f$ hyperfine levels is a good assumption. However, the origin of one x-ray line in the ^{176}Hf spectrum at 1873 keV (see Fig. 2) is not clear. It seems to be a muonic x ray or prompt γ ray of ^{176}Hf and it could be the result of a nuclear resonance.[13] The otherwise good quality of the fit of the hyperfine lines in ^{176}Hf implies that this state does not seriously affect our interpretation and therefore in our subsequent analysis it has been ignored.

In the case of the even-A isotopes, we also fitted the experimental muonic K and L x-ray transition energies[4] with the adjustable parameters mentioned above. The experimental and calculated transition energies and intensities are shown in Table II. The direct spectrum-fitting method and the transition-energy fitting method yielded results that agreed well with each other. Since the transition-energy fitting method is precluded in the case of the odd-A hafnium isotopes because of the complexity of the spectra, we list in this paper, for consistency, only the results of the direct spectrum-fitting method for both even-A and odd-A hafnium isotopes.

IV. NUCLEAR MONOPOLE PARAMETERS

A. Isotope shifts

Muonic x-ray experiments provide information about the nuclear monopole charge radius that can be expressed in terms of the Barrett moment $\langle r^k e^{-\alpha r}\rangle$ (Ref. 14) or the Barrett equivalent radius R_k (Ref. 15). The experimental uncertainties in the monopole Barrett moments can be computed directly from the uncertainties in the measured x-ray energies. A total uncertainty of approximately 800 eV is assigned to the energy of each K x ray [consisting of a quadratic sum of statistical errors ($\lesssim$300 eV), errors due to the nonlinearity of the data-acquisition system ($\lesssim$400 eV), and uncertainties in the nuclear polarization corrections ($\lesssim$600 eV)]. Similarly, a total uncertainty of 300 eV

TABLE IV. Parameters fixed in the analysis of data for odd-A hafnium nuclei.

^{177}Hf		^{179}Hf	
β_2[a]	0.268	β_2[a]	0.257
$E(\frac{9}{2}^-)$ (keV)	112.95	$E(\frac{11}{2}^+)$ (keV)	122.7
$E(\frac{11}{2}^-)$ (keV)	249.67	$E(\frac{13}{2}^+)$ (keV)	268.8
$E(\frac{13}{2}^-)$ (keV)	409.5	$E(\frac{15}{2}^+)$ (keV)	438.6
$E(\frac{15}{2}^-)$ (keV)	591.3	$E(\frac{17}{2}^+)$ (keV)	631.2
$\mu(\frac{7}{2}^-)$[b] (μ_N)	0.79	$\mu(\frac{9}{2}^+)$[b] (μ_N)	−0.64
$\mu(\frac{9}{2}^-)$[b] (μ_N)	1.08	$\mu(\frac{11}{2}^+)$[c] (μ_N)	−0.07
$Q(\frac{11}{2}^-)$[a] (e b)	0.08	$Q(\frac{13}{2}^+)$[a] (e b)	0.70
$Q(\frac{13}{2}^-)$[a] (e b)	−0.72	$Q(\frac{15}{2}^+)$[a] (e b)	−0.14
$Q(\frac{15}{2}^-)$[a] (e b)	−1.27	$Q(\frac{17}{2}^+)$[a] (e b)	−0.73
$B(E2{:}\frac{9}{2}^-\rightarrow\frac{13}{2}^-)$[a] ($e^2b^2$)	0.98	$B(E2{:}\frac{11}{2}^+\rightarrow\frac{15}{2}^+)$[a] ($e^2b^2$)	0.70
$B(E2{:}\frac{11}{2}^-\rightarrow\frac{13}{2}^-)$[a] ($e^2b^2$)	1.77	$B(E2{:}\frac{13}{2}^+\rightarrow\frac{15}{2}^+)$[a] ($e^2b^2$)	1.81
$B(E2{:}\frac{11}{2}^-\rightarrow\frac{15}{2}^-)$[a] ($e^2b^2$)	1.25	$B(E2{:}\frac{13}{2}^+\rightarrow\frac{17}{2}^+)$[a] ($e^2b^2$)	0.94
$B(E2{:}\frac{13}{2}^-\rightarrow\frac{15}{2}^-)$[a] ($e^2b^2$)	1.44	$B(E2{:}\frac{15}{2}^+\rightarrow\frac{17}{2}^+)$[a] ($e^2b^2$)	1.57

[a]Estimated from the ground-state quadrupole moments of Ref. 2 using the rotational model.
[b]*Table of Isotopes,* 7th ed., edited by C. M. Lederer and V. S. Shirley (Wiley, New York, 1977).
[c]Estimated from the strong coupling model.

TABLE V. Monopole charge parameters of hafnium nuclei.

	^{176}Hf	^{177}Hf	^{178}Hf	^{179}Hf	^{180}Hf
Barrett parametrization[a]					
$2p_{1/2}$-$1s_{1/2}$ transition					
$\langle r^k e^{-\alpha r}\rangle$ (fm^k)	2.0286×10^1	2.0321×10^1	2.0383×10^1	2.0439×10^1	2.0471×10^1
R_k (fm)	6.7990(14)	6.8030(14)	6.8107(14)	6.8162(14)	6.8234(14)
k	2.2740	2.2745	2.2753	2.2762	2.2762
C_z (fm/keV)	-1.775×10^{-3}	-1.777×10^{-3}	-1.779×10^{-3}	-1.782×10^{-3}	-1.783×10^{-3}
$2p_{3/2}$-$1s_{1/2}$ transition					
$\langle r^k e^{-\alpha r}\rangle$ (fm^k)	2.0664×10^1	2.0699×10^1	2.0759×10^1	2.0816×10^1	2.0864×10^1
R_k (fm)	6.8001(14)	6.8040(14)	6.8117(14)	6.8172(14)	6.8244(14)
k	2.2847	2.2852	2.2859	2.2868	2.2872
C_z (fm/keV)	-1.710×10^{-3}	-1.711×10^{-3}	-1.714×10^{-3}	-1.716×10^{-3}	-1.718×10^{-3}
$3d_{3/2}$-$2p_{1/2}$ transition					
$\langle r^k e^{-\alpha r}\rangle$ (fm^k)	1.841×10^2	1.874×10^2	1.879×10^2	1.883×10^2	1.880×10^2
R_k (fm)	6.914(5)	6.918(5)	6.923(5)	6.923(5)	6.934(5)
k	3.5261	3.5354	3.5359	3.5369	3.5338
C_z (fm/keV)	-1.541×10^{-2}	-1.540×10^{-2}	-1.540×10^{-2}	-1.542×10^{-2}	-1.540×10^{-2}
$3d_{5/2}$-$2p_{3/2}$ transition					
$\langle r^k e^{-\alpha r}\rangle$ (fm^k)	4.710×10^2	4.714×10^2	4.721×10^2	4.717×10^2	4.739×10^2
R_k (fm)	6.959(7)	6.962(7)	6.966(7)	6.964(7)	6.975(7)
k	4.0456	4.0454	4.0452	4.0453	4.0448
C_z (fm/keV)	-2.292×10^{-2}	-2.291×10^{-2}	-2.290×10^{-2}	-2.292×10^{-2}	-2.287×10^{-2}
Model dependent parametrization[b]					
C (fm)	6.288(2)	6.297(4)	6.317(2)	6.348(4)	6.340(2)
a (fm)	0.519(1)	0.517(3)	0.514(1)	0.498(3)	0.510(1)
$\langle r^2\rangle$ (fm^2)	28.421(23)	28.448(51)	28.497(22)	28.509(51)	28.589(19)

[a]The Barrett moment (Ref. 14), the Barrett radius (Ref. 15), and the sensitivity (Ref. 15) are denoted by $\langle r^k e^{-\alpha r}\rangle$, R_k, and C_z, respectively. The error in R_k was estimated from the energy uncertainty of 800 eV for K x rays and 300 eV for L x rays as discussed in the text. The parameter α in $\langle r^k e^{-\alpha r}\rangle$ is fixed at $\alpha=0.1388$ fm^{-1} (Ref. 18).

[b]The model assumes the deformed Fermi charge distribution with a radius parameter C and a diffuseness parameter a. The error in $\langle r^2\rangle$ is estimated from the derivatives $\delta\langle r^2\rangle/\delta C$ and $\delta\langle r^2\rangle/\delta a$. The errors include only statistical uncertainties.

is estimated for the energy of each L x ray [statistics (≤ 120 eV), nonlinearity (≤ 100 eV), and nuclear polarization (≤ 250 eV)].

The monopole charge parameters deduced from the present experiment are summarized in Table V. The mean-square charge radii $\langle r^2\rangle$, which have been computed from the deformed Fermi charge distributions, are also listed for each isotope. It should be kept in mind, however, an extrapolation from the measured Barrett moments is required to compute $\langle r^2\rangle$ and hence the values deduced from this quantity may contain a model error.

Table VI lists our values for the isotope shifts, together with values from nonmuonic measurements. For the isotope shift calculations, the mean-square charge radii were computed from the Barrett radii using the empirical formula[16] $\langle r^2\rangle^{1/2}=0.782R_k$. The uncertainties listed for the muonic values in Table VI are only those of statistical origin, since other errors cancel to a large extent in computing isotope shifts. The muonic result for the $\Delta N=2$ isotope shift between ^{178}Hf and ^{180}Hf is in good agreement with electronic K x-ray measurements. However, our values do not agree well with the optical measurements.

Figure 5 is a plot of the relative isotope-shift values $\Delta R_{k,\mathrm{exp}}^{\Delta N=2}/\Delta R_{k,\mathrm{std}}^{\Delta N=2}$ vs the neutron number N. The standard isotope shift $\Delta R_{k,\mathrm{std}}=\Delta A/3AR_k$ is that expected for

TABLE VI. Isotope shifts $\Delta\langle r^2\rangle$ for pairs of hafnium nuclei (in fm^2).

Nuclei	Muonic x ray[a]	Optical[b] measurement	e^- K x ray[c]
178–176	0.096(7)	0.065(14)	
180–178	0.106(7)	0.078(16)	0.103(7)
177–176	0.032(9)	0.008(8)	
179–178	0.046(9)	0.031(13)	

[a]Present work. Differences of charge radii $\Delta\langle r^2\rangle$ are estimated from the R_k obtained from the $2p_{3/2}$-$1s_{1/2}$ transition in Table V and the empirical formula $\langle r^2\rangle^{1/2}=0.782R_k$ of Ref. 16. Errors include only statistical uncertainties.

[b]E. Finckh and A. Steudel, Z. Phys. 141, 19 (1955).

[c]S. K. Bhattacherjee, F. Boehm, and P. L. Lee, Phys. Rev. 188, 1919 (1969).

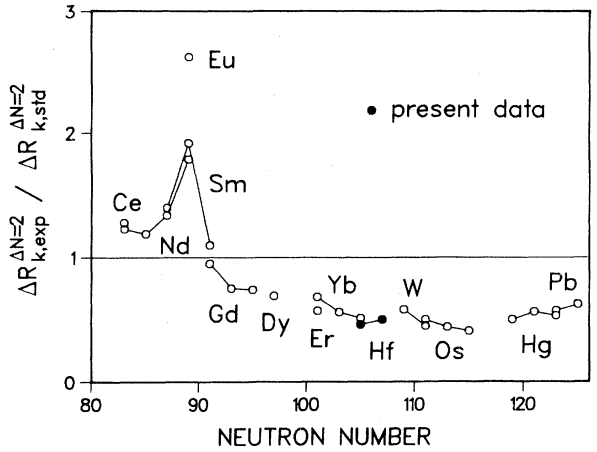

FIG. 5. Summary of the $\Delta N=2$ isotope shifts in the region $N=82-126$. The differences in the Barrett equivalent radii ΔR_k were deduced from the muonic $2p_{3/2}$-$1s_{1/2}$ transitions. The figure includes the present results for hafnium nuclei, data from Refs. 4 and 15–21, and the europium data from Ref. 22.

spherical nuclei with a constant nuclear density. The figure indicates that the $\Delta N=2$ isotope shifts of the even-A hafnium nuclei follow the empirical trend of other isotope shifts in the deformed region.

The $\Delta N=1$ isotope shifts for the series $^{176-178}$Hf show only a weak odd-even staggering, in contrast to the optical results. In terms of the usual staggering parameter,

$$\Gamma_{A+1}=\frac{R_k(A+1)-R_k(A)}{[R_k(A+2)-R_k(A)]/2}\ , \tag{1}$$

the odd-even staggering effect is calculated to be $\Gamma_{177}=0.67(19)$ and $\Gamma_{179}=0.87(17)$, while the optical measurements give $\Gamma_{177}(\text{opt})=0.25(25)$ and $\Gamma_{179}(\text{opt})=0.79(34)$.

It has been suggested[23,24] that odd-even staggering of isotope shifts may be attributed to a staggering in nuclear deformation between odd and even isotopes. However, the odd-even staggering observed in the hafnium isotopes cannot be explained simply by the change of nuclear deformation. If we assume, for example, a volume-conserving deformed Fermi charge distribution[25] (with $C=1.12A^{1/3}$ fm, $a=0.523$ fm, and β_2 from Refs. 1 and 2), the model predicts Γ_{177} to be 1.27(26) and Γ_{179} to be 1.03(20), in disagreement with our experimental results.

B. Isomer shifts of the first 2^+ states

The present analysis yielded isomer-shift energies of the first excited states of the hafnium nuclei. The energy shift arises because the monopole charge distribution of an excited state is, in general, slightly different from that of the ground state. The isomer-shift energies are listed in Table VII, together with previous experimental results.

For a comparison of our results with those of the Mössbauer experiment,[26] the energy shift must be converted into differences of mean-square charge radii $\Delta\langle r^2\rangle$. In the present analysis the energy shifts ΔE_{iso} were first converted to ΔR_k by using the sensitivity values C_z in Table V, and the ΔR_k values were then expressed in terms of $\Delta\langle r^2\rangle$ by using the empirical formula of Ref. 16.

In contrast to the Mössbauer experiment, we derive negative isomer shifts for the even-A hafnium nuclei, implying that the radius of the monopole charge density of the first excited 2^+ state is smaller than the radius of the ground-state charge density of each isotope. The isomer shift is largest for the 2^+ state of ^{176}Hf, a fact that has not been predicted by existing theories.[27,28] This large negative isomer shift of ^{176}Hf is corroborated in the present study by observation of the nuclear deexcitation γ ray from muonic ^{176}Hf. The energy of this γ ray in our spectrum was determined to be 87.517(157) keV, as calibrated by the nearby muonic x rays of ^{12}C (Ref. 29). From the γ-ray energy we deduce an isomer shift energy of $\Delta E_{\text{iso}}=830(160)$ eV (uncorrected for the possible $M1$ hyperfine transition[30]). This value is consistent with that determined from the K x-ray spectra in the present experiment. The isomer shifts of ^{178,180}Hf were also determined by using the deexcitation γ-ray method and the results were found to be in good agreement with those obtained from the muonic x-ray analysis.

The large negative isomer shift of ^{176}Hf suggests that

TABLE VII. Isomer shifts for the first excited state of hafnium nuclei.

	Muonic x rays[a]		Mössbauer[b]	Theory[c]	Theory[d]
Nucleus	ΔE_{iso}[e] (keV)	$\Delta\langle r^2\rangle$[f] (fm^2)	$\Delta\langle r^2\rangle$ (fm^2)	$\Delta\langle r^2\rangle$ (fm^2)	$\Delta\langle r^2\rangle$ (fm^2)
^{176}Hf	−0.63(14)	−0.0090(20)	0.0016	0.0054	−0.0001
^{177}Hf	−0.10(26)	−0.0014(37)			
^{178}Hf	−0.22(13)	−0.0031(18)	−0.0004	0.0038	0.0003
^{179}Hf	0.06(27)	0.0008(38)			
^{180}Hf	−0.12(11)	−0.0016(15)	0.0008	0.0038	0.0010

[a]Present work.
[b]Reference 26.
[c]Reference 27.
[d]Reference 28.
[e]The errors quoted for ΔE_{iso} include only statistical uncertainties.
[f]Differences of charge radii $\Delta\langle r^2\rangle$ are estimated from ΔE_{iso} by using the sensitivity C_z of the $2p_{3/2}$-$1s_{1/2}$ transition in Table V and the empirical formula $\langle r^2\rangle^{1/2}=0.782R_k$ of Ref. 16.

this nucleus is not rigid against nuclear rotations. But neither is ^{176}Hf soft in the manner of ^{152}Sm (Ref. 4) and ^{154}Gd (Ref. 17), whose large positive isomer shifts can be explained by the stretching effect[27,28] of nuclear rotation. Negative isomer shifts, which may be due to the Coriolis antipairing effect of nuclear rotation, have also been observed in the osmium nuclei.[16]

V. NUCLEAR QUADRUPOLE PARAMETERS

The quadrupole parameters that can be extracted from analysis of muonic x-ray spectra are the quadrupole radial integrals W_{E2} defined in Ref. 8. Interpretation of W_{E2} in terms of the spectroscopic quadrupole matrix elements $\langle I'||r^2Y_2||I\rangle$ requires assumption of a model for the transition charge density $\rho_{E2}^{I'I}(r)$. A detailed discussion of this topic has been presented in Refs. 16 and 31.

Our muonic x-ray data for ^{177,179}Hf can provide an estimate of the radial position of the quadrupole charge density since the spectroscopic quadrupole moments of the $\frac{7}{2}^-$ ground state of ^{177}Hf and of the $\frac{9}{2}^+$ ground state of ^{179}Hf are precisely and model-independently known[2] from the hyperfine-splitting energies of the muonic M x rays, namely, $Q_M^{177}=3.365(29)$ e b and $Q_M^{179}=3.793(33)$ e b. The information concerning the transition density is obtained indirectly from a comparison of the M x-ray and the K and L x-ray spectra, because the ground-state quadrupole moments extracted from the latter spectra are sensitive to the transition charge density $\rho_{E2}^{I'I}(r)$ used in the analysis. If we use a transition charge density derived from a deformed Fermi charge distribution, whose radius and diffuseness parameters are determined from the monopole part of the charge density as fitted to experiment, we obtain quadrupole moment values from the K and L x rays that are larger than the M x-ray derived values by 1.9(9)% for ^{177}Hf and by 2.6(9)% for ^{179}Hf.

We therefore adjusted the radius parameter of the quadrupole charge density $\rho_{E2}^{I'I}(r)$ until the quadrupole moment deduced from the muonic K and L x rays became consistent with the quadrupole moment deduced from the muonic M x rays. The radii [see Eq. (22) in Ref. 4] of the quadrupole charge densities are found to be about 0.18 fm smaller than the radii of the monopole charge densities for both ^{177}Hf and ^{179}Hf.

For the even-A hafnium isotopes, no quadrupole information is available from the M x rays and we have therefore assumed the same radial displacement for the quadrupole charge densities as we observed for the odd-A hafnium nuclei; i.e., we assumed that the radii of the quadrupole charge densities are smaller by 0.18 fm than the monopole charge radii.

A combined electron scattering and muonic x-ray analysis[32] has shown that a similarly "diminished" transition charge radius is needed to explain the hyperfine spectra of ^{192}Os. The diminished radius parameter of the transition charge density implies simply that a deformed Fermi charge distribution cannot be the common intrinsic shape from which both the monopole and the quadrupole charge densities are obtained by a multipole expansion.

Tables VIII and IX list the model-independent quadrupole radial integrals W_{E2}, and the spectroscopic quadrupole parameters deduced from the transition charge densities discussed above. A simple rotor model predicts that the ratio of the static to the transition matrix elements for the 2^+ states,

$$R=-\frac{\sqrt{7}W_{E2}^{2^+p_{3/2},2^+p_{1/2}}}{\sqrt{10}W_{E2}^{2^+p_{3/2},0^+p_{1/2}}} \tag{2}$$

is unity. Our measured values essentially agree with this prediction. However, all values R are slightly larger than unity, which seem to be due to the low-lying β-vibrational bands[4] observed in these nuclei.

For the even-A hafnium nuclei the deduced $B(E2)$ values agree satisfactorily with Coulomb excitation data.[1] For the odd-A hafnium nuclei, for which no other experimental data seem to exist, we have compared our results with predictions of the axially symmetric rotor model (Table IX). If the intrinsic quadrupole moment of this

TABLE VIII. Quadrupole parameters of even-A hafnium nuclei.

	^{176}Hf	^{178}Hf	^{180}Hf
Present experiment			
$W^{2^+p_{3/2},2^+p_{1/2}}$ [a] (fm^{-1})	0.1300(5)	0.1248(5)	0.1234(5)
$W^{2^+p_{3/2},0^+p_{1/2}}$ [a] (fm^{-1})	−0.1081(3)	−0.1040(3)	−0.1024(3)
$Q(2^+)$ [b] (e b)	−2.10(2)	−2.02(2)	−2.00(2)
$B(E2{:}0^+\rightarrow 2^+)$ [b] (e^2b^2)	5.29(10)	4.91(10)	4.78(10)
R [c]	1.006(5)	1.004(5)	1.008(5)
Coulomb excitation [d]			
$B(E2{:}0^+\rightarrow 2^+)$ (e^2b^2)	5.20(5)	4.86(5)	4.74(4)

[a]The errors listed for the quadrupole radial integrals W include only statistical errors and an error of 0.3% arising from the uncertainty of the nuclear polarization corrections.
[b]An error of 1% arising from the uncertainty of the radius of the transition charge density is included.
[c]Ratios given by Eq. (2) in the text.
[d]Reference 1.

TABLE IX. Quadrupole parameters of odd-A hafnium nuclei.

	^{177}Hf		^{179}Hf
Present experiment			
$W^{7/2^-p_{3/2},7/2^-p_{1/2}}$[a] (fm^{-1})	−0.2055(7)	$W^{9/2^+p_{3/2},9/2^+p_{1/2}}$[a] (fm^{-1})	−0.2408(8)
$W^{9/2^-p_{3/2},9/2^-p_{1/2}}$[a] (fm^{-1})	−0.0825(12)	$W^{11/2^+p_{3/2},11/2^+p_{1/2}}$[a] (fm^{-1})	−0.1239(12)
$W^{9/2^-p_{3/2},7/2^-p_{1/2}}$[a] (fm^{-1})	−0.1962(7)	$W^{11/2^+p_{3/2},9/2^+p_{1/2}}$[a] (fm^{-1})	−0.2003(7)
$W^{11/2^-p_{3/2},7/2^-p_{1/2}}$[a] (fm^{-1})	−0.0992(8)	$W^{13/2^+p_{3/2},9/2^+p_{1/2}}$[a] (fm^{-1})	−0.0912(11)
$W^{11/2^-p_{3/2},9/2^-p_{1/2}}$[a] (fm^{-1})	−0.2156(12)	$W^{13/2^+p_{3/2},11/2^+p_{1/2}}$[a] (fm^{-1})	−0.2274(13)
$Q(\frac{7}{2}^-)$[b] (e b)	3.35(3)	$Q(\frac{9}{2}^+)$[b] (e b)	3.80(4)
$Q(\frac{9}{2}^-)$[b] (e b)	1.30(2)	$Q(\frac{11}{2}^+)$[b] (e b)	1.88(3)
$B(E2{:}\frac{7}{2}^-\rightarrow\frac{9}{2}^-)$[b] ($e^2$b^2)	2.18(4)	$B(E2{:}\frac{9}{2}^+\rightarrow\frac{11}{2}^+)$[b] ($e^2$b^2)	1.82(4)
$B(E2{:}\frac{7}{2}^-\rightarrow\frac{11}{2}^-)$[b] ($e^2$b^2)	0.56(1)	$B(E2{:}\frac{9}{2}^+\rightarrow\frac{13}{2}^+)$[b] ($e^2$b^2)	0.38(1)
$B(E2{:}\frac{9}{2}^-\rightarrow\frac{11}{2}^-)$[b] ($e^2$b^2)	2.11(5)	$B(E2{:}\frac{11}{2}^+\rightarrow\frac{13}{2}^+)$[b] ($e^2$b^2)	1.96(4)
Symmetric rotor model			
Q_0 [$Q(\frac{7}{2}^-)$ of Ref. 2]	7.21(6)	Q_0 [$Q(\frac{9}{2}^+)$ of Ref. 2]	6.95(6)
$Q(\frac{9}{2}^-)$ (e b)	1.31(1)	$Q(\frac{11}{2}^+)$ (e b)	1.91(2)
$B(E2{:}\frac{7}{2}^-\rightarrow\frac{9}{2}^-)$ (e^2b^2)	2.19(4)	$B(E2{:}\frac{9}{2}^+\rightarrow\frac{11}{2}^+)$ (e^2b^2)	1.81(4)
$B(E2{:}\frac{7}{2}^-\rightarrow\frac{11}{2}^-)$ (e^2b^2)	0.56(1)	$B(E2{:}\frac{9}{2}^+\rightarrow\frac{13}{2}^+)$ (e^2b^2)	0.37(1)
$B(E2{:}\frac{9}{2}^-\rightarrow\frac{11}{2}^-)$ (e^2b^2)	2.13(4)	$B(E2{:}\frac{11}{2}^+\rightarrow\frac{13}{2}^+)$ (e^2b^2)	2.00(4)

[a]The errors listed for the quadrupole radial integrals W include only statistical errors and an error of 0.3% arising from the uncertainty of the nuclear polarization corrections.

[b]An error of 1% arising from the uncertainty of the radius of the transition charge density is included.

model is determined from the spectroscopic moment of the ground state, the predicted quadrupole moment of the first excited state and the $B(E2)$ values agree satisfactorily with experiment.

By using a technique developed in Ref. 33, inelastic electron scattering data can be accurately normalized with the quadrupole radial integrals W_{E2} in Tables VIII and IX. This technique involves fitting the muon-generated potential $V_{E2}^{j'j}(r)$ to the analytic form[8] $r^2(A+Br^me^{-\alpha r})$.

TABLE X. Muon generated quadrupole potential parameters obtained by fitting $V_{E2}^{p_{3/2},p_{1/2}}(r)$ to the form $r^2(A+Br^me^{-\alpha r})$. The parameters m and α are fixed at 2.3125 and 0.1399, respectively (Ref. 8).

	A (fm^{-3})	B (fm^{-m-3})
^{176}Hf	-7.791×10^{-4}	9.420×10^{-6}
^{177}Hf	-7.790×10^{-4}	9.420×10^{-6}
^{178}Hf	-7.789×10^{-4}	9.419×10^{-6}
^{179}Hf	-7.789×10^{-4}	9.419×10^{-6}
^{180}Hf	-7.787×10^{-4}	9.418×10^{-6}

For convenience in using the normalization procedure, we list in Table X the coefficients involved in this expression.

VI. SUMMARY AND CONCLUSIONS

The monopole and quadrupole charge parameters of $^{176-180}$Hf have been investigated by means of muonic x-ray experiments. In general, the quadrupole moments and $B(E2)$ values of the low-lying states of these nuclei agree satisfactorily with predictions of the axially symmetric rotor model. However, certain deviations from the model have been revealed.

The isomer shifts of the first excited 2^+ states of ^{176,178,180}Hf are negative. The especially large negative isomer shift of the 2^+ state of ^{176}Hf has not been predicted by existing theories. The quadrupole charge radii of the ground-state quadrupole moments of ^{177}Hf and ^{179}Hf are smaller by about 0.18 fm than the respective monopole charge radii. This fact implies that, as the intrinsic charge distribution, a deformed Fermi charge distribution is not adequate to explain the muonic x rays of the odd-A hafnium isotopes.

The above facts are in contrast to observations of samarium and gadolinium which have positive isomer shifts for the 2^+ states of the even-A isotopes, and where

a deformed Fermi charge distribution adequately explains the muonic x-ray spectra. We concluded that the hafnium nuclei, even though their electric quadrupole parameters are reasonably well explained by the axially symmetric rotor model like those of samarium and gadolinium, possess properties of the γ-soft rotors in the osmium region.

ACKNOWLEDGMENTS

All work was carried out at Los Alamos National Laboratory. One of the authors (W.R.) was supported in part by Deutscher Akademischer Austauschdienst, Bonn, Federal Republic of Germany. This work was supported by the U.S. Department of Energy.

[1]R. M. Ronningen, J. H. Hamilton, L. Varnell, J. Lange, A. V. Ramayya, G. Garcia-Bermudez, W. Lourens, L. L. Riedinger, F. K. McGowan, P. H. Stelson, R. L. Robinson, and J. L. C. Ford, Jr., Phys. Rev. C 16, 2208 (1977).
[2]Y. Tanaka, R. M. Steffen, E. B. Shera, W. Reuter, M. V. Hoehn, and J. D. Zumbro, Phys. Rev. Lett. 51, 1633 (1983).
[3]E. B. Shera, E. T. Ritter, R. B. Perkins, G. A. Rinker, L. K. Wagner, H. D. Wohlfahrt, G. Fricke, and R. M. Steffen, Phys. Rev. C 14, 731 (1976).
[4]Y. Yamazaki, E. B. Shera, M. V. Hoehn, and R. M. Steffen, Phys. Rev. C 18, 1474 (1978).
[5]E. B. Shera, the program XRAY3 (unpublished).
[6]D. Kessler, H. Mes, A. C. Thompson, H. L. Anderson, M. S. Dixit, C. K. Hargrove, and R. J. McKee, Phys. Rev. C 11, 1719 (1975).
[7]M. V. Hoehn and E. B. Shera (unpublished).
[8]L. K. Wagner, E. B. Shera, G. A. Rinker, and R. K. Sheline, Phys. Rev. C 16, 1549 (1977).
[9]Y. Tanaka, the programs MUON2 and XRAY2 (unpublished).
[10]G. A. Rinker, Comput. Phys. Commun. 16, 221 (1979).
[11]G. A. Rinker and R. M. Steffen, At. Data Nucl. Data Tables 20, 143 (1977).
[12]J. M. McKinley (unpublished). An explicit form of this correction can be found in Ref. 20.
[13]M. V. Hoehn and E. B. Shera, Phys. Rev. C 20, 1934 (1979).
[14]R. C. Barrett, Phys. Lett. 33B, 388 (1970).
[15]K. W. Ford and G. A. Rinker, Phys. Rev. C 7, 1206 (1973).
[16]M. V. Hoehn, E. B. Shera, H. D. Wohlfahrt, Y. Yamazaki, R. M. Steffen, and R. K. Sheline, Phys. Rev. C 24, 1667 (1981).
[17]D. B. Laubacher, Y. Tanaka, R. M. Steffen, E. B. Shera, and M. V. Hoehn, Phys. Rev. C 27, 1772 (1983).
[18]R. Engfer, H. Schneuwly, J. L. Vuilleumier, H. K. Walter, and A. Zehnder, At. Data Nucl. Data Tables 14, 509 (1974).
[19]R. J. Powers, P. Barreau, B. Bihoreau, J. Miller, J. Morgenstern, J. Picard, and L. Roussel, Nucl. Phys. A316, 295 (1979).
[20]A. Zehnder, F. Boehm, W. Dey, R. Engfer, H. K. Walter, and J. L. Vuilleumier, Nucl. Phys. A254, 315 (1975).
[21]A. A. Hahn, J. P. Miller, R. J. Powers, A. Zehnder, A. M. Rushton, R. E. Welsh, A. R. Kunselman, P. Roberson, and H. K. Walter, Nucl. Phys. A314, 361 (1979).
[22]Y. Tanaka, R. M. Steffen, E. B. Shera, W. Reuter, M. V. Hoehn, and J. D. Zumbro, Phys. Rev. C 29, 1897 (1984).
[23]L. Wilets, D. L. Hill, and K. W. Ford, Phys. Rev. 91, 1488 (1953).
[24]B. S. Reehal and R. A. Sorensen, Nucl. Phys. A161, 385 (1971).
[25]M. Brack, T. Ledergerber, H. C. Pauli, and A. S. Jensen, Nucl. Phys. A234, 185 (1974).
[26]G. M. Kalvius and G. K. Shenoy, At. Data Nucl. Data Tables 14, 639 (1974).
[27]E. R. Marshalek, Phys. Rev. Lett. 20, 214 (1968).
[28]J. Meyer and J. Speth, Nucl. Phys. A203, 17 (1973).
[29]L. A. Schaller, L. Schellenberg, A. Ruetschi, and H. Schneuwly, Nucl. Phys. A343, 333 (1980).
[30]A. Gal, L. Grodzins, and J. Hufner, Phys. Rev. Lett. 21, 453 (1968).
[31]Y. Tanaka, R. M. Steffen, E. B. Shera, W. Reuter, M. V. Hoehn, and J. D. Zumbro, Phys. Rev. C 29, 1830 (1984).
[32]W. Reuter, E. B. Shera, M. V. Hoehn, F. W. Hersman, T. Milliman, J. M. Finn, C. Hyde-Wright, R. Lourie, B. Pugh, and W. Bertozzi, Phys. Lett. 137B, 32 (1984).
[33]W. Reuter, E. B. Shera, H. D. Wohlfahrt, and Y. Tanaka, Phys. Lett. 124B, 293 (1983).